Inorganic Chemistry
Communication

Inorg. Chem. **2010**, *49*, 7617–7619 **7617**
DOI: 10.1021/ic100580g

Slow Magnetic Relaxation in an Octanuclear Manganese Chain

Chen-I Yang,[†,‡] Shao-Po Hung,[†] Gene-Hsiang Lee,[§] Motohiro Nakano,[∥] and Hui-Lien Tsai*[,†]

[†]*Department of Chemistry, National Cheng Kung University, Tainan 701, Taiwan,* [‡]*Institute of Chemistry, Academia Sinica, Taipei 115, Taiwan,* [§]*Instrumentation Center, College of Science, National Taiwan University, Taipei 106, Taiwan, and* [∥]*Division of Applied Chemistry Graduate School of Engineering, Osaka University, 2-1 Yamada-oka, Suita 565-0871, Japan*

Received March 28, 2010

A one-dimensional chain containing a mixed-valence octanuclear manganese(II,III) building unit, $(NEt_4)_{2n}[Mn_8O_2(salox)_6(N_3)_8(MeOH)_3]_n$ (H_2salox = salicylaldoxime), was synthesized and characterized structurally and magnetically. Each building unit contains a $[Mn^{II}_2Mn^{III}_6O_2]^{18+}$ structural topology. The frequency dependence of the out-of-phase component in alternating current magnetic susceptibilities and hysteresis loops for the complex indicates single-chain-magnet-like behavior.

The development of new magnetic materials based on molecules is one of the most important research topics in the chemistry and physics fields. Single-molecule magnets (SMMs) and single-chain magnets (SCMs) have attracted a lot of attention because they exhibit quantum phenomena[1] and finite-size effects[2] and because of their possible applications as nanometric magnetic memory units.[3] The first reported SCM was $[Co(hfac)_2\{NIT(C_6H_4OMe)\}]$ [hfac = hexafluoroacetylacetonate; NIT(R) = 2-(4-R)-4,4,5,5-tetramethylimidazoline-1-oxyl-3-xoide], which has a spiral one-dimensional (1D) isolated chain structure.[4] Because of the presence of anisotropic Co^{II} metal ions, this chain has been described as an Ising chain; it displays hysteresis behavior at low temperatures without undergoing three-dimensional magnetic ordering. The slow dynamics of magnetization was explained using Glauber's model[5] for Ising spin chains. The physics underlying this system has motivated the synthesis of new SCMs.[6] Polynuclear manganese clusters have received considerable interest as building blocks for 1D chains of SCMs because they often exhibit large, and sometimes abnormally large, spin values in the ground state and have a large anisotropy.[7] The end-on bridging azide ligands often mediate ferromagnetic exchange between paramagnetic centers; this property has recently been exploited in the preparation of SMMs and SCMs.[8,9]

The present study reports a new structural type of 1D chain, composed of $[Mn_8O_2(salox)_6(N_3)_8(MeOH)_3]^{2+}$ building units

*To whom correspondence should be addressed. E-mail: hltsai@mail.ncku.edu.tw.

(1) (a) Thomas, L.; Lionti, F.; Ballou, R.; Gatteschi, D.; Sessoli, R.; Barbara, B. *Nature* **1996**, *383*, 145. (b) Friedman, J. R.; Sarachik, M. P.; Tejada, J.; Ziolo, R. *Phys. Rev. Lett.* **1996**, *76*, 3830. (c) Wernsdorfer, W.; Sessoli, R. *Science* **1999**, *284*, 133. (d) Wernsdorfer, W.; Aliaga-Alcalde, N.; Hendrickson, D. N.; Christou, G. *Nature* **2002**, *416*, 406.

(2) (a) Lecren, L.; Roubeau, O.; Coulon, C.; Li, Y.-G.; Le Goff, X. F.; Wernsdorfer, W.; Miyasaka, H.; Clérac, R. *J. Am. Chem. Soc.* **2005**, *127*, 17353. (b) Yoo, J.; Wernsdorfer, W.; Yang, E.-C.; Nakano, M.; Rheingold, A. L.; Hendrickson, D. N. *Inorg. Chem.* **2005**, *44*, 3377.

(3) (a) Suzuki, M.; Kubo, R. *J. Phys. Soc. Jpn.* **1968**, *24*, 51. (b) Stanley, R. *Phase Transition and Critical Phenomena*; Clarendon Press: Oxford, U.K., 1971; Appendix E, p 280.

(4) Caneschi, A.; Gatteschi, D.; Lalioti, N.; Sangregorio, C.; Sessoli, R.; Venturi, G.; Vindigni, A.; Rettori, A.; Pini, M. G.; Novak, M. A. *Angew. Chem., Int. Ed.* **2001**, *40*, 1760.

(5) Glauber, R. J. *J. Math. Phys.* **1963**, *4*, 294.

(6) (a) Clérac, R.; Miyasaka, H.; Yamashita, M.; Coulon, C. *J. Am. Chem. Soc.* **2002**, *124*, 12837. (b) Palii, A. V.; Reu, O. S.; Ostrovsky, S. M.; Klokishner, S. I.; Tsukerblat, B. S.; Sun, Z.-M.; Mao, J.-G.; Prosvirin, A. V.; Zhao, H.-H.; Dunbar, K. R. *J. Am. Chem. Soc.* **2008**, *130*, 14729. (c) Przybylak, S. W.; Tuna, F.; Teat, S. J.; Winpenny, R. E. P. *Chem. Commun.* **2008**, 1983. (d) Bernot, K.; Luzon, J.; Sessoli, R.; Vindigni, A.; Thion, J.; Richeter, S.; Leclercq, D.; Larionova, J.; van der Lee, A. *J. Am. Chem. Soc.* **2008**, *130*, 1619. (e) Coulon, C.; Miyasaka, H.; Clérac, R. *Struct. Bonding* (*Berlin*) **2006**, *122*, 163. (f) Miyasaka, H.; Julve, M.; Yamashita, M.; Clérac, R. *Inorg. Chem.* **2009**, *48*, 3420 and references cited therein. (g) Coulon, C.; Clérac, R.; Wernsdorfer, W.; Colin, T.; Yamashita, M. *Phys. Rev. Lett.* **2009**, *102*, 167204. (h) Harris, T. D.; Bennett, M. V.; Clérac, R.; Long, J. R. *J. Am. Chem. Soc.* **2010**, *132*, 3980. (i) Miyasaka, H.; Takayama, K.; Saitoh, A.; Furukawa, S.; Yamashita, M.; Clérac, R. *Chem.—Eur. J.* **2010**, *16*, 3656.

(7) (a) Chakov, N. E.; Wernsdorfer, W.; Abboud, K. A.; Christou, G. *Inorg. Chem.* **2004**, *43*, 5919. (b) Brockman, J. T.; Stamatatos, T. C.; Wernsdorfer, W.; Abboud, K. A.; Christou, G. *Inorg. Chem.* **2007**, *46*, 9160. (c) Milios, C. J.; Inglis, R.; Vinslava, A.; Prescimone, A.; Parsons, S.; Perlepes, S. P.; Christou, G.; Brechin, E. K. *Chem. Commun.* **2007**, 2738. (d) Jones, L. F.; Prescimone, A.; Evangelisti, M.; Brechin, E. K. *Chem. Commun.* **2009**, 2023. (e) Milios, C. J.; Vinslava, A.; Whittaker, A. G.; Parsons, S.; Wernsdorfer, W.; Christou, G.; Perlepes, S. P.; Brechin, E. K. *Inorg. Chem.* **2006**, *45*, 5275. (f) Stoumpos, C. C.; Inglis, R.; Roubeau, O.; Sartzi, H.; Kitos, A. A.; Milios, C. J.; Aromi, G.; Tasiopoulos, A. J.; Nastopoulos, V.; Brechin, E. K.; Perlepes, S. P. *Inorg. Chem.* **2010**, *49*, 4388.

(8) (a) Murugesu, M.; Habrych, M.; Wernsdorfer, W.; Abboud, K. A.; Christou, G. *J. Am. Chem. Soc.* **2004**, *126*, 4766. (b) Ako, A. M.; Hewitt, I. J.; Mereacre, V.; Clérac, R.; Wernsdorfer, W.; Anson, C. E.; Powell, A. K. *Angew. Chem., Int. Ed.* **2006**, *45*, 4926. (c) Stamatatos, T. C.; Abboud, K. A.; Wernsdorfer, W.; Christou, G. *Angew. Chem., Int. Ed.* **2007**, *46*, 884. (d) Yang, C.-I.; Wernsdorfer, W.; Lee, G.-H.; Tsai, H.-L. *J. Am. Chem. Soc.* **2007**, *129*, 456.

(9) (a) Liu, T.-F.; Fu, D.; Gao, S.; Zhang, Y.-Z.; Sun, H.-L.; Su, G.; Liu, Y. J. *J. Am. Chem. Soc.* **2003**, *125*, 13976. (b) Pardo, E.; Ruiz-García, R.; Lloret, F.; Faus, J.; Julve, M.; Journaux, Y.; Delgado, F.; Ruiz-Pérez, C. *Adv. Mater.* **2004**, *16*, 1597. (c) Stamatatos, T. C.; Abboud, K. A.; Wernsdorfer, W.; Christou, G. *Inorg. Chem.* **2009**, *48*, 807. (d) Xu, H. B.; Wang, B. W.; Pan, F.; Wang, Z. M.; Gao, S. *Angew. Chem., Int. Ed.* **2007**, *46*, 7388.

Published on Web 08/13/2010

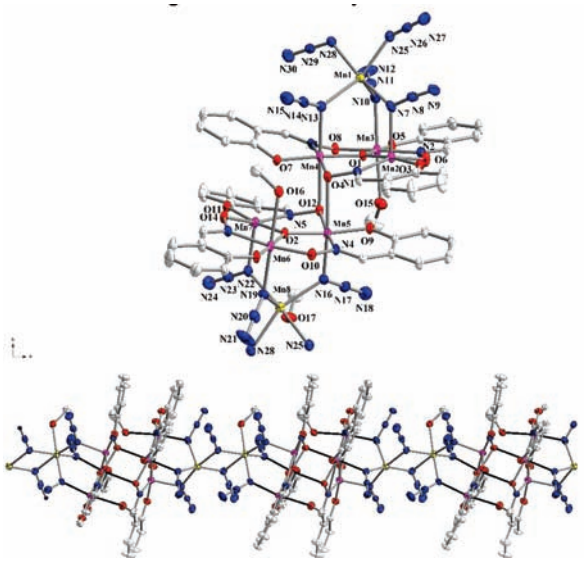

Figure 1. (Top) ORTEP drawing of **1** with thermal ellipsoids set at 30% probability. (Bottom) Structure of the 1D chain. The solvent molecules, H atoms, and NEt_4^+ ions have been omitted for clarity.

bridged by end-on azides, that exhibits slow relaxation of magnetization and hysteresis effects.

The reaction of $Mn(NO_3)_2 \cdot 4H_2O$ (1 equiv), sodium azide (2 equiv), and salicylaldoxime (H_2salox; 1 equiv) with NEt_4OH (1 equiv) in MeOH at room temperature yielded a deep-green solution. Et_2O was slowly diffused into the resulting solution to form dark-green crystals of $(NEt_4)_{2n}[Mn_8O_2(salox)_6(N_3)_8(MeOH)_3]_n \cdot 1.5n$MeOH (**1**·1.5MeOH) in a yield of 53%.

The structure of one Mn_8 unit of the chain **1** is shown in Figure 1. Complex **1** crystallizes in monoclinic space group $P2_1/c$.[10] The structure of each Mn_8 unit contains a nonplanar $[Mn^{III}_6(\mu_3\text{-}O^{2-})_2(\mu_3\text{-}OR)_2]^{12+}$ unit of two offset, stacked $[Mn^{III}_3(\mu_3\text{-}O^{2-})]^{7+}$ triangular subunits linked by two central oximato O atoms, with each triangle having Mn^{II}, Mn1, and Mn8 attached by three $\mu\text{-}N_3^-$ ions. Two more azide ligands are bonded terminally to the Mn^{II} ions and connect octanuclear clusters in one dimension along the *a* axis in the end-on coordination mode. Charge considerations of complex **1** require $2Mn^{II}$ and $6Mn^{III}$ oxidation state descriptions. Mn1 and Mn8 are assigned as Mn^{II} ions, whereas Mn2, Mn3, Mn4, Mn5, Mn6, and Mn7 are assigned as Mn^{III} ions based on the fact that (i) the average bond lengths of Mn2−Mn7 are longer than those of Mn1 and Mn8 and (ii) bond valence sum (BVS) calculations give values that are in good agreement with the above assignments (Table 2S in the Supporting Information). The Mn ions can be divided into four groups: four Mn^{III} ions (Mn3, Mn4, Mn5, and Mn6) with six-coordination, two Mn^{III} ions (Mn2 and Mn7) with square-pyramidal five-coordination, one Mn^{II} ion (Mn1) with square-pyramidal five-coordination, and one Mn^{II} ion (Mn8) with six-coordination. Peripheral ligations around the core are provided by four $salox^{2-}$ groups in their familiar $\eta^1{:}\eta^1{:}\eta^1{:}\mu_2$ binding modes, two $salox^{2-}$ groups in the fairly rare $\eta^1{:}\eta^1{:}\eta^2{:}\mu_3$ mode, and six N_3^- ligands in the $\eta^2{:}\mu_2$ mode; three MeOH molecules complete the sixth coordination position around Mn3, Mn6, and Mn8. The six-coordination Mn^{III} ions have Jahn−Teller (JT) distortions in axes elongation along N10−Mn3−O15, N13−Mn4−O12, N16−Mn5−O4, and N19−Mn6−O16. The JT elongation axes are aligned nearly parallel to each other in the Mn_8 unit. The mean directions of the JT axes of each Mn_8 unit and chain directional axis are staggered at ca. 17° (Figure 1S in the Supporting Information). In addition, the chains are well isolated by two NEt_4^+ cations with no hydrogen bonding or $\pi-\pi$ interaction.

(10) Satisfactory elemental analytical data for $(NEt_4)_2[Mn_8O_2(salox)_6(N_3)_6(MeOH)_3]\cdot 1.5$MeOH. Calcd: C, 37.11; H, 4.38; N, 22.16. Found: C, 36.68; H, 4.29; N, 22.23. Crystal data for **1**·1.5MeOH: $C_{62.5}H_{88}Mn_8N_{32}O_{18.5}$, M = 2023.17, monoclinic, $P2_1/n$, a = 13.6118(4) Å, b = 24.9565(8) Å, c = 25.1167(8) Å, β = 99.608(2)°, V = 8412.5(5) Å^3, T = 150(2) K, Z = 4, R (R_w) = 0.0645 (0.1407).

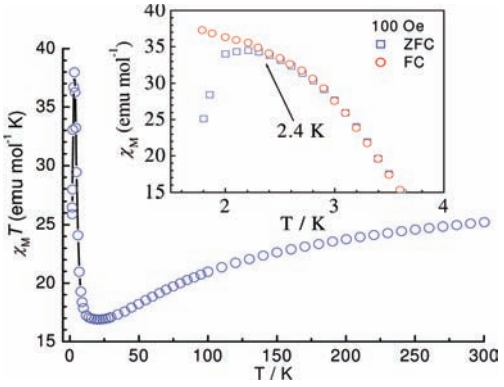

Figure 2. Plots of $\chi_M T$ vs T for **1**·1.5MeOH in an applied field of 1 kG from 1.8 to 300 K. Inset: FC and ZFC magnetization for **1**·1.5MeOH in an applied field of 100 G.

Solid-state, variable-temperature magnetic susceptibility measurements were performed on microcrystalline samples of complex **1**·1.5MeOH (suspended in eicosane to prevent torquing) in the 1.8−300 K range in a 1 kG magnetic field. The temperature dependence of $\chi_M T$ of **1**·1.5MeOH is shown in Figure 2. The $\chi_M T$ value at 300 K is 25.2 emu mol^{-1} K, slightly lower than the 26.76 emu mol^{-1} K value expected for two Mn^{II} and six Mn^{III} ions with g = 2.0. The $\chi_M T$ value decreases upon cooling to a minimum of 16.9 emu K mol^{-1} at 22 K, indicating the presence of dominant antiferromagnetic exchange interactions within the Mn_8 cluster. It then increases to a maximum of 38.0 emu K mol^{-1} at 3.5 K, followed by a rapid decrease to 25.9 emu mol^{-1} K at 1.8 K. The inverse of the direct-current (dc) susceptibility decreases linearly from 300 to 100 K, roughly following Curie−Weiss behavior with C = 26.3 emu mol^{-1} K and θ = −28.1 K (Figure 2S in the Supporting Information). The Curie constant is in good agreement with the spin-only value of 26.76 emu mol^{-1} K for six Mn^{III} (S = 2) and two Mn^{II} ($S = {}^5/_2$) ions with an average g value of 2. The negative Weiss constant indicates that the dominant interaction between spin carriers is antiferromagnetic. Because of the topological complexity of Mn_8, the individual pairwise manganese exchange interactions cannot be determined using the Kambe method. The sharp increase of $\chi_M T$ at temperatures below 8 K is a characteristic of the ferromagnetic behavior. The long Mn−Mn separations between the chains (>9 Å) imply weak dipole—dipole interactions between adjacent chains, suggesting 1D behavior of the ferromagnetic interaction of each Mn_8 unit. This is reasonable because $[M_2(\mu_{1,1}\text{-}N_3)_2]$ usually displays ferromagnetic interaction at M−N−M angles < 105°; the angle of Mn−N−Mn in complex **1**·1.5MeOH is ca. 103°.[11] Moreover, the magnetic susceptibility of irreversibility in the field-cooled (FC) and zero-field-cooled (ZFC) plots is around 2.4 K (Figure 2, inset).

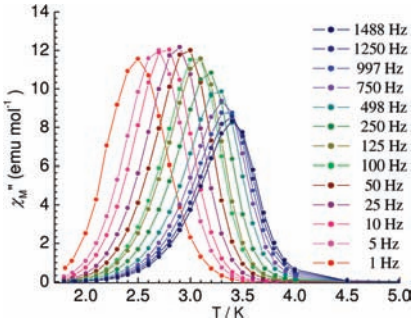

Figure 3. Plot of χ_M'' vs temperature for a microcrystalline sample of complex **1**·1.5MeOH under a zero dc field and an ac field of 3.5 G. The data were collected in an ac field oscillating at the indicated frequencies.

Alternating-current (ac) susceptibility measurements were performed on a microcrystalline sample of complex **1**·1.5MeOH in a 3.5 G ac field oscillating at 1−1488 Hz and under a zero dc field. The in-phase ($\chi_M'T$) signals showed frequency dependence (decreasing below $T = 4.0$ K), which is indicative of the onset of slow magnetic relaxation (Figure 3S in the Supporting Information). The out-of-phase (χ_M'') signals increased with decreasing temperature, reaching the maximum value at 2.5−3.4 K and then approaching zero; these signals are also frequency-dependent. The plots of χ_M'' vs T are shown in Figure 3. When the frequency of the ac field was changed from 1488 to 1 Hz, the χ_M'' peak shifted from 3.4 to 2.5 K. These data indicate a significant barrier to magnetization relaxation and preclude 3D ordering.[6c,9c] The peak temperatures of χ_M' can be measured by the parameter $\phi = (\Delta T_p/T_p)/\Delta(\log f) = 0.08$, which is close to the range of normal superparamagnets.[12,13] The Arrhenius equation was applied to a fit of the data to obtain the rate of reversal of magnetization and the effective energy barrier of the molecule. The plot of the relaxation time as a function of the inverse of temperature for complex **1**·1.5MeOH is shown in Figure 4S in the Supporting Information. The figure shows the presence of a crossover between two different activated regimes, both of which give best fits with two different barriers and physical τ_0 values ($\Delta_{\tau_1} = 64$ K and 1.7×10^{-12} s and $\Delta_{\tau_2} = 79$ K and 7.4×10^{-15} s for the low- and high-temperature regimes, respectively). The effective energy barrier and τ_0 are close to those found in a previous study on SCMs.[9a,14] The crossover in the Arrhenius plot of SCMs has been predicted to be due to finite-size effects[15] and for systems with a slow relaxation of single monomeric units.[16] The plot of $\ln(\chi_M'T)$ vs $1/T$ shows a linear increase between 3.1 and 4.5 K with an energy gap of $\Delta_\xi = 14.5$ K (Figure 5S in the Supporting Information), which is consistent with the difference between the two energy barriers ($\Delta_{\tau_2} - \Delta_{\tau_1}$).[17] Furthermore, at a fixed temperature of 2.9 K and a zero applied magnetic field, a semicircle Cole−Cole diagram was obtained. The diagram can be fitted by a generalized Debye model[18] with an α parameter of 0.33, which indicates a moderate distribution of the relaxation time (Figure 6S in the Supporting Information).

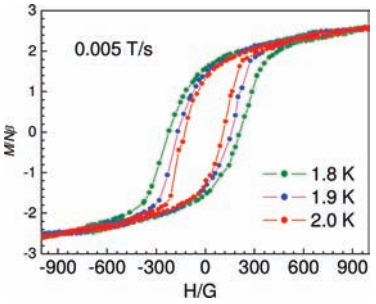

Figure 4. Magnetization vs field hysteresis loop measurement of **1**·1.5MeOH at the indicated temperatures at a 0.005 T s^{-1} scan rate.

The assignment of **1**·1.5MeOH as an SCM was further confirmed by the field dependence of magnetization, which was measured in the temperature range of 1.8−2.0 K (Figure 4). The width of the loops is strongly temperature-dependent (increasing with decreasing temperature), as expected for the superparamagnetic-like behavior observed for SCMs.

In summary, an infinite-chain complex was built up using octanuclear mixed-valence $Mn^{II,III}$ units with N_3^- and N,O-donor ligands of salicylaldoximate, which linked to form the chain structure with $\eta^2{:}\mu^2$ end-on N_3^-. The frequency dependence of the ac signals and magnetization hysteresis loop suggest that complex **1**·1.5MeOH is a new SCM.

Acknowledgment. The magnetic measurements were obtained from SQUID (MPMS XL-7) at NSYSU. Financial support by the National Science Council of Taiwan (Grant NSC-96-2113-M-006-010-MY3) is gratefully acknowledged.

Supporting Information Available: Crystallographic details in CIF format, BVS values, and magnetism data. This material is available free of charge via the Internet at http://pubs.acs.org.

(11) Ribas, J.; Escuer, A.; Monfort, M.; Vicente, R.; Cortés, R.; Lezama, L.; Rojo, T. *Coord. Chem. Rev.* **1999**, *193*−*195*, 1027.
(12) (a) Ferbinteanu, M.; Miyasaka, H.; Wernsdorfer, W.; Nakata, K.; Sugiura, K.; Yamashita, M.; Coulon, C.; Clérac, R. *J. Am. Chem. Soc.* **2005**, *127*, 3090. (b) Bernot, K.; Bogani, L.; Caneschi, A.; Gatteschi, D.; Sessoli, R. *J. Am. Chem. Soc.* **2006**, *128*, 7947.
(13) $\phi = 0.01$ is a typical value for a spin glass. For details, see: Mydosh, J. A. *Spin Glasses: An Experimental Introduction*; Taylor & Francis: London, 1993.
(14) (a) Wang, S.; Zuo, J.-L.; Gao, S.; Song, Y.; Zhou, H.-C.; Zhang, Y.-Z.; You, X.-Z. *J. Am. Chem. Soc.* **2004**, *126*, 8900. (b) Toma, L. M.; Lescouëzec, R.; Lloret, F.; Julve, M.; Vaissermann, J.; Verdaguer, M. *Chem. Commun.* **2003**, 1850.
(15) (a) da Silva, J. K. L.; Moreira, A. G.; Soares, M. S.; Barreto, F. C. S. *Phys. Rev. E* **1995**, *52*, 4527. (b) Luscombe, J. H.; Luban, M.; Reynolds, J. P. *Phys. Rev. E* **1996**, *53*, 5852.
(16) Coulon, C.; Clérac, R.; Lecren, L.; Wernsdorfer, W.; Miyasaka, H. *Phys. Rev. B* **2004**, *69*, 132408.
(17) Vindigni, A.; Rettori, A.; Bogani, L.; Caneschi, A.; Gatteschi, D.; Sessoli, R.; Novak, M. A. *Appl. Phys. Lett.* **2005**, *87*, 073102.
(18) (a) Cole, K. S.; Cole, R. H. *J. Chem. Phys.* **1941**, *9*, 341. (b) Aubin, S. M. J.; Sun, Z.; Pardi, L.; Krzystek, J.; Folting, K.; Brunel, L.-C.; Rheingold, A. L.; Christou, G.; Hendrickson, D. N. *Inorg. Chem.* **1999**, *38*, 5329.